Molar wear in house mice: insight into diet preferences at an ecological timescale?

Sabrina Renaud, Ronan Ledevin, Anne-Béatrice Dufour, Caroline Romestaing, Emilie Hardouin

Molar wear in house mice: insight into diet preferences at an ecological time scale?

Sabrina Renaud[1], Ronan Ledevin[2], Anne-Béatrice Dufour[1], Caroline Romestaing[3], Emilie A. Hardouin[4]

[1] Laboratoire de Biométrie et Biologie Evolutive (LBBE), UMR 5558 CNRS, Université Claude Bernard Lyon 1, Université de Lyon, Villeurbanne, France

[2] De la Préhistoire à l'Actuel : Culture, Environnement et Anthropologie (PACEA), UMR 5199 CNRS, Université de Bordeaux, Pessac, France

[3] Univ Lyon, Université Claude Bernard Lyon 1, CNRS, ENTPE, UMR 5023 LEHNA, F-69622, Villeurbanne, France

[4] Department of Life and Environmental Sciences, Faculty of Sciences and Technology, Bournemouth University, Poole, UK

ORCID ID

Sabrina Renaud: 0000-0002-8730-3113

Ronan Ledevin: 0000-0002-1936-9612

Anne-Béatrice Dufour: 0000-0002-9339-4293

Caroline Romestaing: 0000-0002-6877-9626

Emilie A. Hardouin: 0000-0002-2031-5160

Running head

Molar wear in house mice

Abstract

In molars without permanent eruption, wear deeply modifies the geometry of the crown. To test for a signature of diet on wear dynamics, the molar geometry was compared between commensal house mice, relying on an omnivorous-granivorous diet, and Sub-Antarctic relatives, characterized by a switch towards a more "predator" behavior. Lab-bred offspring of commensal mice served as reference by providing mice of known age. Molar geometry was quantified using dense 3D semi-landmarks based descriptors of the whole molar row and the upper molar only.

Lab offspring displayed decreased rate of wear compared to their commensal relatives, due to reduced mastication in mice fed *ad libitum.* Sub-Antarctic mice displayed a similarly decreased rate of molar wear, in agreement with an optimization towards incisor biting to seize preys. Lab offspring and Sub-Antarctic mice were further characterized by straight molar rows, whereas in commensal mice, the erupting third molar was deviated away from the longitudinal alignment with the other molars, due to masticatory loadings.

Quantifying changes in molar geometry could thus contribute to trace subtle diet variations, and provide a direct insight into the constraints during mastication, shedding light on the functional role of adaptive changes in molar geometry.

Keywords

Geometric morphometrics – Kerguelen Archipelago – Mastication – Molar crown geometry – *Mus musculus domesticus* – Occlusal relief – Subantartic environment.

Introduction

Mammalian teeth are very diverse in their morphology, allowing the consumption of various food items. As such, the evolution of the mammalian dental pattern participated to the radiation of the group (Hunter & Jernvall, 1995; Grossnickle et al., 2019), leaving both a phylogenetic (Cucchi et al., 2017) and an ecological signal (Gómez Cano et al., 2013) on tooth morphology. In teeth without permanent eruption, wear is the only factor modifying this geometry after dental eruption. Being the consequence of both abrasion, due to the contact of the tooth with the food items, and attrition, due to tooth-tooth contact, wear considerably affects the crown geometry. As a consequence, wear can be considered as being problematic by overprinting the original morphology and thus obliterating other signals, including genetic differences in tooth shape (Ledevin et al., 2016; Pallares et al., 2017). Conversely, wear depends on masticatory behavior and on the food items consumed along an animal's life (Teaford & Oyen, 1989) and has thus the potential to trace ecological variations on a very short time scale. Teeth are often the only fossil remain for small mammals such as rodents. Retrieving fine-scale ecological information from their geometry could be precious for understanding the selective pressure acting on their evolution (Gomes Rodrigues et al., 2013).

Among rodents, the house mouse (*Mus musculus domesticus*) has been associated with humans even before the Neolithic (Weissbrod et al., 2017). Being unintentional fellow-travelers of human exchanges allowed house mice to be one of the most successful invader worldwide (Cucchi, 2008; Jones et al., 2012). As such, mice have been confronted to a variety of diets depending on local resources (Miller & Webb; Le Roux et al., 2002). Being also easily bred in laboratory condition, the house mouse constitutes a good model to test for signature of diet differences in both wild and experimental conditions.

Experiments on a laboratory strain demonstrated that hard and soft eaters differed in the rate of molar wear (Renaud & Ledevin, 2017). Comparison between mice trapped in the wild and relatives bred in the lab further showed that the alignment of the molars on the jaw is impacted by loadings during mastication, with wild mice showing a torsion of the molar row not observed in their lab offspring (Savriama et al., 2022). Lab mice being bred with unlimited access to food, they presumably chewed less thoroughly than wild mice confronted to the cost of foraging. If so, wild populations differing in diet may display similar differences in wear trajectories and molar insertion. The present study therefore focuses on the comparison between commensal mice and Sub-Antarctic populations from the Kerguelen archipelago. In such Sub-Antarctic environments, mice shifted their diet from their usual omnivorous-granivorous diet to a larger proportion of terrestrial animal prey (Le Roux et al., 2002). This triggered an optimization of their jaw morphology for incisor biting, crucial for seizing

prey (Renaud et al., 2015b). Functional performance for molar mastication was concomitantly decreased, suggesting a relaxation of the functional demand compared with commensal mice feeding on anthropic resources, especially grains in agricultural settings.

The geometric signature of wear, and more generally of use, on the molar system may thus have the potential to trace fine-scale differences in diet between populations. Commensal mice from different populations should share similar wear rates. In Sub-Antarctic mice, for which incisor biting is predominant and masticatory loadings reduced, rate of wear and torsion of the molar row should be reduced, similarly to what is observed in lab-bred mice.

The signature of wear on the molar system has been quantified using a dense 3D quantification of the molar morphology (Renaud et al., 2018b; Savriama et al., 2022) on three complementary descriptors: the complete molar row (UMR), the first molar (UM1) and a truncated template of the UM1 (UM1tr), corresponding to the part of the crown affected by wear only late in life. Considering the truncated UM1 should allow to focus on genetic differences between populations (Ledevin et al., 2016; Pallares et al., 2017). The analysis of the complete crown of the first upper molar provides information relative to wear, whereas the geometry of the molar row further includes the relative arrangement of the three molars along the row. It may also vary depending on the relative size of the three molars. Molars develop according to a developmental cascade, the first molar inhibiting the subsequent ones. The increase in relative size of the first molar to the detriment of the third molar has been suggested as a signature of faunivorous diet (Kavanagh et al., 2007). This component of geometric variation of the molar row has therefore been investigated as well.

Material

The material is composed of three sets of the Western European house mouse subspecies (*Mus m. domesticus*) (Supp. Fig. 1; Supp. Table 1).

(1) Commensal house mice were documented by two French populations. Nineteen mice were trapped in a horse stable in Balan, nearby Lyon (group later on designed as Balan Wild). A second set of ten commensal house mice was trapped in two neighboring farms in Tourch (Brittany, France) (Renaud et al., 2017).

(2) Non-commensal Sub-Antarctic mice were sampled on the small Guillou Island (Kerguelen Archipelago, Indian Ocean), including nine mice from 1993 and eleven mice from 2009 (Renaud et al., 2015b). This sampling brackets a period of important human-driven environmental modifications on Guillou Island that changed the resources available to the house mice. The rabbit (*Oryctolagus*

cuniculus) constituted an important competitor until its eradication by poisoning in 1994 (Chapuis et al., 2001). During the subsequent recovery from rabbit grazing, invasive plants progressed against native vegetation in relation to climate change (Chapuis et al., 2004). Invertebrate prey constitutes an important component in the diet of Guillou mice (Le Roux et al., 2002), but earthworm availability in the litter decreased over the period due to increasing summer drought (Lebouvier et al., 2002) whereas native insects regressed due to the spread of an invasive carabid predator (*Merizodus soledadenus*) (Laparie et al., 2010).

(3) Lab-bred mice corresponded to offspring of mice trapped in Balan and brought alive to the animal facility ACSED (Lyon University). After approximately two months of acclimation, the wild-trapped mice were paired to obtain F1 offspring that were bred with standard rodent pellets (SAFE A04), with food and water *ad libitum*. Some of these F1 mice were paired to obtained F2 descendants. Breeding was conducted in accordance with animal care guidelines. This dataset included 22 laboratory descendants ranging from one to four months of age, plus one young mouse at weaning (21 days of age). This group is designed as Balan Lab.

Body weight data were available for all mice. Age and sex were available for all Balan Lab mice, except sex for the young mouse at 21 days.

All mice were killed according to the directive 2010/63/UE of the European Parliament on the protection of animals used for scientific purposes.

Methods

Acquisition and extraction of 3D surfaces

Most skulls were scanned at a cubic voxel resolution of 12 µm using similar settings. Wild mice from Balan, Tourch and most laboratory offspring were scanned on the General Electric (GE) Nanotom microtomograph (µCT) of the AniRA-ImmOs platform of the SFR Biosciences, Ecole Normale Supérieure (Lyon, France). Skulls from Guillou were scanned at the PACEA laboratory (Bordeaux, France) using a similar equipment (GE v tome x s) at a resolution of 12 µm. The dataset was complemented by one Balan Wild scanned at 12 µm and eight Balan Lab scanned at 17 µm at the Mateis laboratory (INSA, Lyon, France), using a similar equipment.

For each mouse, the right upper molar row (UMR) was segmented using Avizo (v. 7.1—Visualization Science Group, FEI Company). In many cases, an automatic threshold was sufficient to isolate the molar row from the surrounding bone and generate a surface including the roots, but in some cases,

connections with the bone had to be manually delimited. Starting from the model of the complete upper molar row, the first upper molar was manually delimited by removing the contact with the second molar. In one case (G93-24), the right molar row was damaged and the mirror image of the left molar row was considered.

The 3D surfaces of seven Balan wild mice and 13 lab offspring are available from a previous study (Renaud et al., 2021). The molar row surfaces corresponding to Tourch and Guillou have been further deposited in MorphoMuseuM (Renaud et al., 2023). Information about the scanned specimens can be found in Supp. Table 1.

Estimates of body size: Body weight and mandible size

Body size. - Body weight was available for all mice, providing an estimate of growth stage. Since weight is more related to volume than to linear size, its cubic root was considered in all analyses.

Mandible size. – For each mouse, a 3D model of the mandible was segmented, in most case considering the right mandible. The 3D length of the mandible was measured as the distance between two landmarks located at posteriormost extremity of the condyle and the anteriormost edge of the mandibular bone along the incisor lingual side. This measure was selected because it can be assessed even on damaged mandibles, and because mandible size has been shown to display very little sexual dimorphism and to be well correlated to body size (head + body length) (Renaud et al., 2017). Landmarks were positioned using MorphoDig (Lebrun, 2018).

3D surfacic description of the molars

Mouse molars are composed of cusps arranged in transverse chevrons (Fig. 1) that are used as rasps to grind food items. Labial, central and lingual cusps align to form three longitudinal rows that guide the forwardly directed motion (propalinal movement) during chewing. This complex geometry can be described using surfacic templates covering the erupted part of the teeth (Ledevin et al., 2016; Renaud & Ledevin, 2017). Three templates were considered, corresponding to (1) the upper molar row (UMR), with the three molars in contact; (2) the first upper molar (UM1) only and (3) a truncated "wear-free" template of the UM1 (UM1tr). These templates, used in a previous study (Savriama et al., 2022), have been empirically elaborated on a specimen of intermediate age (Balan Lab #86). "Wear-free" templates, designed on other reference molars, were successful in discarding wear effect to focus on genetic differences in various contexts (Ledevin et al., 2016; Pallares et al., 2017).

The young mouse at 21 days could not be included in the analysis of the molar row, since the third molar, erupting at weaning, was not yet in contact with the second one.

The templates were used to extract cropped surfaces limited to the zone of interest. Fixed landmarks were used to guide the application of the template on each of the initial surfaces. Five landmarks were located on the UM1, one at the anterior front of the molar, two in lateral valleys (between cusps t1 and t4 on the lingual side, and between t3 and t6 on the labial side (see Fig. 1 for nomenclature of the cusps) and two in the valleys bracketing the median cusps t5. Being located low on the crown, they could be used both for the complete UM1 and the truncated template. Six additional landmarks (three on the second molar and three on the third molar) were collected to anchor the template of the molar row. Fixed landmarks were manually positioned using MorphoDig (Lebrun, 2018). Sets of equally spaced sliding semi-landmarks were then projected on the cropped surfaces using the package Rvcg (Schlager, 2017), leading to 2186 semi-landmarks for the UMR, 2199 for the UM1 and 2293 for the UM1tr (Fig. 1) (Savriama et al., 2022).

The sliding procedure for these semi-landmarks was done using the minimum bending energy criterion (Bookstein, 1997). A generalized Procrustes analysis (GPA) was applied to the semi-landmarks, leading to shape descriptors (the aligned coordinates) by removing the effects of location, orientation, and position. The sliding procedure and the GPA were performed using the Morpho package (Schlager, 2017).

Relative size of the first and third molars

The 3D area or volume of molars includes the degree of abrasion of the cusps. The relative area of the first vs third molar was thus evaluated on 2D projections of the occlusal surface, that are less impacted by wear. The cropped surfaces of the molar row were oriented with the occlusal surface facing up. On snapshots of this view, the first, second and third molars were manually delineated. The areas of the three molars were then automatically extracted using the image analyzing software Optimas. The first / third molar area ratio estimated the relative size of the two teeth.

Statistical analyses

Regarding univariate estimators, differences between groups (Balan Wild, Balan Lab, Tourch, Guillou 1993, and Guillou 2009) were tested using non-parametric Kruskal–Wallis tests complemented by pairwise Wilcoxon tests. Linear regressions and Pearson correlations were used to test for

covariation between variables. Analyses of variance (ANOVA) were used to test for the effect of age and sex on size estimators in the Balan Lab group. Similarly, Procrustes ANOVAs were used to investigate the effect of age and sex on the molar geometry within the Balan Lab group. Since no effect of sex was documented on molar geometry, and because sexual dimorphism has been repeatedly shown to be absent or reduced when considering molar size and shape in house mice (Valenzuela-Lamas et al., 2011; Renaud et al., 2017), males and females were pooled in all subsequent analyses.

The shape information was first summarized by Principal Component Analyses (PCA) applied to variance-covariance matrix of the aligned coordinates using the package Morpho. Differences between the five groups were tested using permutational MANOVA performed on the Procrustes distances (Procrustes ANOVA) using the package geomorph (Adams & Otarola-Castillo, 2013). Relationship between shape (aligned coordinates) and proxies of body size were investigated using Procrustes ANOVA using a model including size, group and their interaction. In all cases, probabilities were based on 9999 permutations. These analyses also provided a regression score summarizing the shape variance along the factors of the model; reconstruction of extreme shapes along the regression scores were performed using geomorph.

The PCA analyses the total variance in a sample (**T**). This variance can be decomposed in two components: the between-group matrix **B** and the within-group matrix **W**. A between-group PCA corresponds to the eigenanalysis of **B** whereas a within-group PCA corresponds to the analysis of **W** that equals **T**–**B** (Dolédec & Chessel, 1987). These analyses are implemented in the package ade4 (Thioulouse et al., 2018) and were used to focus on between-group differences on the one hand, and on the pattern of within-group variance on the other hand. However, between-group PCAs (later bgPCA) are sensitive to problems of "over-fitting" when too many variables are included compared to the number of specimens, leading to representations where groups appear much more distinct than they really are (Cardini et al., 2019; Thioulouse et al., 2021). To insure a realistic representation of the differentiation between groups, cross-validated factor maps were considered, validated by permutational tests of between-group differences (randtest, 9999 permutations); the index of spuriousness ΔOij was further evaluated (Thioulouse et al., 2021).

A multivariate regression was used to remove the signal attributable to genetic differences from the UMR and UM1 variation. The scores on the first two axes of the PCA on the truncated UM1 were considered to summarize the shape differentiation from genetic origin; the aligned coordinates of the UMR and of the UM1 were regressed on these two UM1tr PC axes to obtained residuals

coordinates that should only contain information relevant to non-genetic variation (wear for the UM1 and UMR, cumulated to the relative arrangement of the molars for the UMR).

Finally, the relationship between inter-individual multivariate topologies based on the UM1 and the UMR was assessed using a coinertia analysis. This method evaluates the concordance between two PCAs in a multivariate way, by finding orthogonal vectors (i.e., co-inertia axes) maximizing the sum of squared covariances between two datasets (Dolédec & Chessel, 1994) and allowing their projection in a common space. This analysis was performed using ade4 (Thioulouse et al., 2018).

All analyses were performed under R (R Core Team, 2018).

Results

Variation in 3D molar geometry

3D geometry of the upper molar row (UMR). – The morphospace corresponding to the upper molar row (Fig. 2A) shows an important within-group variance and a differentiation between populations. The within-group variance is oblique along PC1 and PC2, but mostly expressed along PC1 (35.4% of total variance). This axis corresponds, towards PC1 positive values, to a flattening of the cusps due to increasing abrasion, and to an increasing curvature of the molar row, with the second and third molar departing from the alignment with the UM1. The differences between the wild populations of Balan Wild, Tourch and Guillou are expressed along PC2 (15.3%). This axis also describes some molar row curvature and features regarding basic cusp morphology, such as the relative development of the posterior labial cusp t9, more pronounced towards PC2 positive values.

Balan Wild mice display an important variation, from unworn to worn-down molar rows where the second and third molars have been pushed towards the lingual side. In contrast, Guillou mice display relatively straight and unworn molar rows, with a reduced variation in the degree of wear, to the exception of one mouse from 2009 displaying a worn-down morphology similar to the ones observed in Balan Wild. Tourch molars are intermediate in morphology and in amount of variation along PC1. Balan Lab displays a molar row morphology intermediate between Balan Wild and Guillou mice.

The UM1 / UM3 relative 2D area did not differ between populations ($P = 0.6189$).

3D geometry of the first upper molar (UM1). – The analysis of the first upper molar (Fig. 2B) provided a pattern close to the one based on the complete molar row. The morphospace based on the first two PC axes shows an important within-group variation along PC1 (51.5%), running parallel in the

different populations and corresponding to a flattening of the cusps, culminating in the five molars with almost completely abraded cusps. In contrast with results based on the UMR, Balan Lab mice plot within the range of their wild relatives (Balan Wild). Guillou mice are differentiated along PC2 (10.2%), due to their divergence in tooth morphology. The commensal population from Tourch appears as intermediate between Balan Wild and Guillou.

3D geometry of the "wear-free" first upper molar (truncated UM1). – The morphological variance appears to be less concentrated on PC1 (21.9% only), that does not describe within-group variance but the morphological difference between the three genetically distinct groups (Balan Wild and Lab, Tourch and Guillou) (Fig. 2C). The second axis (PC2, 13.6%) mostly corresponds to a pattern of within-group variation opposing molars with an extended vs short forepart. Despite using the truncated "wear-free" template, four out of five teeth with highly advanced wear appear as outliers in the morphospace, showing that the cusp geometry is too much erased to deliver relevant information regarding genetic differences.

Variation in body and molar size

All populations displayed similar body weight$^{1/3}$ (Fig. 3A, Table 1) and differences are reduced regarding mandible length (Fig. 3B). The pattern was quite different regarding tooth size, with significant differences involving Guillou mice (Table 1). These mice tended to display smaller teeth than the Western European ones (Fig. 3C).

Mandible length increased with body weight$^{1/3}$ (Fig. 3D), with a significant effect of populations but no interaction (Weight$^{1/3}$ $P < 0.0001$, population $P < 0.0001$, interaction $P = 0.327$), meaning that the slopes were not different between populations. The relationship was shifted in Guillou 1993 (Fig. 3D), with smaller mandibles than expected for a given weight. Considering separate Pearson correlation per population, the relationship between mandible length and weight$^{1/3}$ was significant in Balan Wild, Balan Lab, Guillou 1993 and Guillou 2009 ($p < 0.0001$). Molar centroid size was in contrast not related to body weight$^{1/3}$ but differed between populations (Weight$^{1/3}$ $P = 0.1411$, population $P < 0.0001$, interaction $P = 0.0733$).

Characterizing wear trajectories

In order to avoid issues due to missing data or outlying specimens, the mouse at weaning and the five senescent mice were discarded, leading to a common sampling of 64 mice for the UMR, the UM1 and the UM1tr.

PCA were performed on these three reduced datasets (Fig. 4) and the variance explained by the "population" factor was estimated using Procrutes ANOVA and between-group PCAs. Compared to the initial sampling, the within-group variance is reduced (Fig. 4A) and remains expressed on PC1 only for the UM1. Difference between populations were highly significant (P = 0.0001) and explained ~30% of the total variance (% of variance related to between-group differences: UMR 32.7%, UM1 27.9%, UM1tr 29.5%; same percentages obtained using Procrutes ANOVA and bgPCAs).

Wear trajectories, age, sex, and body size in the laboratory population. - A first approach to identify the role of wear in the geometric variation of the molars was to performed Procrustes ANOVA on the aligned coordinates using a proxy of the animal's growth as covariate. Such analyses provide regression scores allowing to visualize the shape variation occurring within each group along the animal's growth (Figs. 5, 6). This method was first applied to the group Balan Lab alone, for which the age of the mice was known. Effect of sex and covariation between age and body size proxies were further investigated, taking advantage of the experimental design (Table 2, Fig. 5). Age but not sex significantly affected molar geometry and proxies of body size, although sex appears to have a marginal effect on body weight$^{1/3}$, males reaching larger size than females in this sample (Fig. 5C).

The UMR geometry was highly influenced by age (Procrustes ANOVA of the aligned coordinates vs age: effect = 15.2%, P = 0.0003). However, the relationship was not linear, with a pronounced change in the geometry of the molar row occurring soon after weaning (Fig. 5A). The change in the geometry of the UM1 is more progressive (Fig. 5B), leading to a higher percentage of variance explained by age (35.7%, P = 0.0001). Similar results were obtained using the cubic root of body weight$^{1/3}$ (UMR: 17.5%, P = 0.0001; UM1: 23.8%, P = 0.0001) or mandible length (UMR: 19.7%, P = 0.0001, UM1: 26%, P = 0.0001) instead of age, showing that these proxies can be used to describe wear trajectories in wild populations, for which mouse age is unknown. However, body weight$^{1/3}$ (Fig. 5C) as mandible length (Fig. 5D) do not display regular increases along age. Both display a rapid growth from weaning until 40 – 60 days of age, then decelerating to almost reach a plateau.

Wear trajectories in the different populations. – Wear trajectories were then assessed in all populations, using Procrustes ANOVA on the aligned coordinates vs a proxy of the animal's growth as

covariate; results were overall similar when using body weight$^{1/3}$ or mandible length as proxy (Table 3). The impact of growth was highly significant ($P < 0.001$) and explained ~7% of shape variation for the upper molar row and the first upper molar. The relationships were not significant when considering the truncated template of the UM1, confirming that wear effects were successfully discarded. Models including growth proxy and population as factors indicated no interaction when considering body weight$^{1/3}$, and no or weak interaction when considering mandible length, showing that the groups shared similar wear trajectories.

Wear trajectories were thus represented using body weight$^{1/3}$ as a proxy of age (Fig. 6). For the UMR as the UM1, despite non-significant interaction term, the slope tended to be steeper in commensal populations (Balan Wild, Tourch) than in Guillou mice; Balan Lab plotted together with the Sub-Antarctic populations. UMR shape changes related to body weight$^{1/3}$ were represented separately in a commensal and a Sub-Antarctic population, taking Balan Wild and Guillou 1993 as examples (Fig. 6A). In both populations, the shape variation associated with increasing body weight$^{1/3}$ corresponded to an abrasion of the cusps, more pronounced along the lingual side. The lingual cusps being initially higher than their labial counterparts, this differential abrasion tend to re-equilibrate the labial and lingual sides of the crown. The component of molar row curvature is present in the wear trajectory of Balan Wild, even in stages corresponding to the smallest animals; in contrast, the molar row from Guillou remains straight whatever the life stage. The UM1 shape variation related to body weight$^{1/3}$ corresponds to an abrasion of the cusps (Fig. 6B).

Wear effect as within-group variation

An alternative approach was to decompose the total shape variance (Fig. 4) into its between- and within-group components. Between-group differentiation was significant in all cases (randtest $P = 0.0001$). Due to the important amount of between-group variation (bgPCA: UMR 32.7%; UM1 27.9%; UM1tr 29.5%), the spurious-group effect induced by the high number of variables was moderate (spuriousness index ΔOij UM1 = 7.9%) to low (ΔOij UMR = 3.2%; ΔOij UM1tr = 2.1%). For the UMR (Fig. 7A) as the UM1 (Fig. 7B), the bgPCA opposed the commensal population of Balan Wild to Sub-Antarctic Guillou populations along a first bgPC axis representing ~70% of between-group variance, with the commensal population of Tourch being intermediate. The main difference regarded the position of Balan Lab, shifted away from their wild relatives for the UMR but plotting in the same range of the morphospace for the UM1. The morphospace corresponding to the truncated UM1 (Fig. 7C) opposed Balan (Wild + Lab) to Guillou (1993 + 2009) along the first axis (bgPC1, 62.1%). The population of Tourch was still intermediate along bgPC1 and differentiates along bgPC2 (23.4%).

The first axis of within-group variance was correlated to body weight$^{1/3}$ regarding the UMR (R = 0.564, P < 0.0001) and the UM1 (R = 0.452, P = 0.0002) but not for the UM1tr (P = 0.8949). The resulting patterns were highly similar to those obtained with the regressions scores, with commensal populations (Balan Wild and Tourch) sharing a trajectory of higher wear for a given weight compared to Guillou mice (Fig. 7D, E). Balan Lab was close to the Sub-Antarctic trajectories. Scores along the first axis of within-group variance were highly correlated to regression scores for the UMR (R = 0.883, P < 0.0001) and the UM1 (R = 0.980, P < 0.0001), underlining that shape variation related to wear corresponded to the main component of shared within-group variance when the complete crown is considered.

Removing the "genetic" signal: regression against UM1tr

A last approach was to consider that the analysis of the truncated UM1 summarized the genetically-driven shape differences among populations. A multivariate regression of the aligned coordinates of the UMR and of the UM1 was performed against the scores on the first two axes of the UM1tr PCA (Fig. 4C) to remove this "genetic" effect and concentrate on wear patterns. A PCA on the resulting residuals aligned coordinates showed, for the UMR, an overlap of Guillou 1993 with Balan Lab, whereas Guillou 2009 plotted with the two commensal populations Balan Wild and Tourch (Fig. 8A).

The first axis of the PCAs on the residuals coordinates was highly correlated to the regression scores (UMR R = 0.900, P < 0.0001; UM1 R = 0.969, P < 0.0001) and to the first within-group PC axes (UMR R = 0.990, P < 0.0001; UM1 R = 0.942, P < 0.0001).

Beyond wear only: Contrasting the response of the molar row and the first upper molar

From the preceding results, the effect of wear could be characterized as shared patterns of within-group shape variation. This does not include all the "use-related" signal, however, since the analysis of the upper molar row shows between-group differences that are neither of genetic origin nor related to wear *sensu stricto*. To better characterize this non-genetic effect beyond wear, the topology obtained for the UMR (Fig. 4A) was compared to the reference topology of the UM1 (Fig. 4B) using a coinertia analysis (Fig. 8B). Arrows show the difference in topology for a given specimen from the first to the second morphospace considered. Compared to the UM1 pattern, including wear, the UMR shows a divergence of Balan Wild away from their laboratory relatives (Balan Lab) and even further away from the Sub-Antarctic populations, while Balan Lab mice were shifted in the

direction of these Sub-Antarctic populations. UMR from Guillou 1993 tended to diverge away from all other populations, including their 2009 relatives.

Discussion

The three-dimensional morphometric analyses of the upper molars showed that the impact of wear was massive and pervasive, when considering the complete molar row as well as when focusing on the first upper molar. Molar wear includes two aspects: attrition due to tooth-tooth contact, and abrasion *sensu stricto* due to the contact of the tooth with food items. Attrition may vary with the masticatory behavior, with possible differences between populations in relation with their usual diet, while abrasion should depend directly from the resources ingested. Both may contribute to a signature of diet on the cusp morphology. Since mice of different age occur in wild-trapped populations, variations in the degree of molar wear overwhelmed the differentiation of genetic origin between the populations. Focusing on the lowest part of the crown by using a truncated template appeared as an efficient way to mitigate this issue, and to focus on genetic differences (Ledevin et al., 2016; Pallares et al., 2017). In contrast, focusing on the upper molar row or the complete UM1 sheds light on processes related to wear and its relationship with diet.

A genetic signature on molar crown shape

Focusing on the genetic signature by using the truncated descriptor of the UM1, molars of the non-commensal mice from Guillou appeared well differentiated from their Western European relatives, in agreement with an important founder effect and subsequent evolution in isolation (Hardouin et al., 2010). Subtler shape differences differentiated the two French commensal populations from Balan and Tourch. These results are in agreement with the fact that house mouse populations function as relatively isolated demes (Pocock et al., 2004), promoting morphological diversification even at a small geographic scale (Chevret et al., 2021). Within-group variation was still important when considering the truncated descriptors of the UM1, but instead of describing molar abrasion, this signal corresponded mostly to changes in the shape of the molar forepart, a signature of developmental variability in house mice (Hayden et al., 2020).

Similar results were already obtained using 2D analyses of the crown outline: divergence between Guillou and European mice (Renaud et al., 2013), differentiation among commensal Western European populations (Renaud et al., 2017) and importance of the molar elongation in within-group variation (Renaud et al., 2011). The facility and low cost of 2D morphometric analyses facilitate

427 access to large sample sizes, useful to assess patterns of within-group variance and their importance
428 in channeling evolution (Renaud et al., 2015a). By suppressing large parts of the tooth geometry, the
429 truncated descriptor of the UM1 operates an important simplification of the tooth geometry, ending
430 close to a description of the two-dimensional molar outline. Yet, it can bring information on the
431 central cusps on the tooth and more details on the shape changes of individual cusps, thus having the
432 potential to provide a useful complement to extensive 2D analyses (Ledevin et al., 2016).

433

434 *Dynamics of wear and molar arrangement through age*

435 The lab-bred group provided the opportunity to investigate the dynamics of wear in controlled
436 conditions, in animals with a wild genetic background. The dynamics observed for the upper molar
437 row was marked by a major change occurring between 26 and 30 postnatal days. In house mice, the
438 third molar is erupting at 21 days, considered as the moment of weaning. In agreement, the young
439 mouse at 21 days displayed an erupting third molar that was not yet in contact with the second
440 molar. Between 22 and 26 days, the third molar was in contact with the second molar but still on the
441 course of eruption, with very poorly developed roots. An abrupt change in geometry corresponded
442 to the termination of the third molar eruption and the achievement of the "adult" arrangement of
443 the three molars along the row. Thereafter, the changes in geometry were less important and
444 followed a linear trajectory, corresponding to the progressive abrasion of the molar cusps.

445 In contrast, the first upper molar (UM1) is only affected by wear *sensu stricto*. As a consequence, its
446 trajectory along age mostly corresponded to a linear trend describing cusp abrasion. The youngest
447 specimens (below 30 days) however appear slightly shifted away from the trend, suggesting two
448 phases, as for the molar row. This may correspond, shortly after weaning, to the onset of the wear
449 facets formation.

450 The shift from milk suckling to mastication is associated with a cohort of anatomical changes,
451 including in the composition of the tongue and masseter muscle fibers. A shift towards muscles with
452 greater contraction speed and force (Maejima et al., 2005) leads to a rapid increase in bite force
453 (Ginot et al., 2020). The weaning period is further associated with a stabilization of mandible shape
454 close to the adult morphology (Swiderski & Zelditch, 2013; Ginot et al., 2020), pointing to a
455 maturation of the whole masticatory apparatus during this critical period. The dynamics observed in
456 the lab may however be modulated in wild mice. Weaning in lab mice was strictly completed at 21
457 postnatal days by removing the litter from the mother. However, in natural conditions, weaning
458 occurs more progressively, with an increasing incorporation of solid food starting at 17 days, and a

cessation of sucking by 23 days, but this date can be modulated depending on nutrient availability and litter size (König & Markl, 1987).

After the weaning phase, the wear facets will progressively expand as the cusps are worn down, up to a point of advanced abrasion resulting in outlying, senescent molar morphologies, that were not observed in the present lab-bred samples nor in laboratory mice aged of six months (Renaud & Ledevin, 2017). Such morphologies were however observed in the two wild populations of Balan and Guillou 2009.

Relationship of wear trajectories with proxies of growth

Age is unknown for wild mice, making the use of indirect proxies necessary to investigate the dynamics of wear across populations. Body size, estimated by weight, and mandible size were considered here. Both continue to grow along the animal's life, without reaching a real plateau (Ginot et al., 2020), making them adequate to trace trajectories along life. However, pace of growth is not linear, slowing down between 40 and 60 postnatal days (this study, (Ginot et al., 2020)). Furthermore, body weight displays a marked sexual dimorphism (Ginot et al., 2020), whereas molar geometry and wear do not. Sexual dimorphism is very limited regarding mandible size (Renaud et al., 2010; Ginot et al., 2020). However, mandible growth can vary across populations, for instance due to nutrient quality, as exemplified by Guillou mice from 1993 displaying a mandible smaller than expected given their body weight (Renaud et al., 2015b). Furthermore, between-group differences in body size, for instance due to insular gigantism (Gray et al., 2015), may render the comparison of trajectories difficult. Each proxy is therefore prone to biases that may distort the image of wear trajectories across populations.

Diet modulates the arrangement of the molars along the row

When comparing the pattern of shape differences obtained on the molar row to those observed for the first upper molar, a component can be isolated that does not correspond to genetic differences (assessed by the analysis of the truncated UM1) nor to wear *sensu stricto* (included in the analysis of the UM1) (Fig. 7). This component corresponds to the arrangement of the three molars along the row. The two commensal populations from Balan and Tourch appear to share a similar signature, with a third molar pushed away from the alignment with the first and second molar towards the lingual side. In contrast, the early Sub-Antarctic population (Guillou 1993) displays a straight molar row.

Murine rodents are characterized by a propalinal masticatory movement (Lazzari et al., 2008), meaning that the grind food by sliding their molar teeth from back to front. The longitudinal alignment of the cusps is of primary functional importance to guide this movement. The torsion observed in the molar rows of the commensal mice shows that the masticatory movement is more complex and incorporates transverse components. In agreement, analysis of jaw motion during mastication showed that the closing movement consists of an arched, forward trajectory (Utsumi et al., 2010) that may contribute to push the third molar towards the lingual side. The onset of differences in molar alignment between commensal and Guillou seems to occur as early as weaning. Since the third molar is just erupting at this time, with not fully developed roots, loadings during mastication could easily modify its insertion relative to the second molar.

The torsion of the molar row in the commensal populations therefore suggest important masticatory loadings, in agreement with a hard diet mostly based on cereal grains, promoting an optimization of the mandible morphology for mastication at the molars (Renaud et al., 2015b). In contrast, Guillou mice have shifted their diet towards an increased proportion of animal prey (Le Roux et al., 2002). This has favored an optimization of the jaw for incisor biting while relaxing the constraints related to mastication (Renaud et al., 2018a), thus limiting the loading on the third molar which can retain its alignment with the first and second ones. Note that, on the short time scale involved, the reduction of the third molar, interpreted as a further signature of faunivorous diet (Kavanagh et al., 2007), did not evolve in these populations.

Strikingly, Balan laboratory offspring display a different molar row geometry compared to their wild relatives. This difference, occurring over one or two generations only, provides evidences that plastic remodeling of the molars' insertion is involved here. The molar geometry of the laboratory offspring tends to converge towards the Guillou one. A similar decrease in masticatory demand likely occurs in lab-bred mice: being fed *ad libitum*, they probably chew their food less thoroughly than wild animals confronted to the costs of foraging (Savriama et al., 2022).

However, the molar row geometry of the most recent population from Guillou, trapped in 2009, appears to share features with commensal mice. Between 1993 and 2009, Guillou Island experienced a cohort of environmental changes that decreased the availability in earthworms but increased the proportion of invasive insects and plants (Lebouvier et al., 2002; Laparie et al., 2010). This presumably led to a more omnivorous diet in mice from 2009 than in those from 1993, a hypothesis supported by changes in mandible shape and slight differences in microwear patterns (Renaud et al., 2015b). This shows that changes in the relative arrangement of the molars along the row can

respond to fine changes in the diet composition on a very small time scale, hardly traceable using alternate proxies of diet.

Wear trajectories suggest reduced abrasion rate in Sub-Antarctic mice

Wear massively affects molar geometry but corresponds to a pattern of within-group variation shared by all populations. Whatever the food consumed, the wear pattern on the first molar seems thus to be comparable. Differently from the early closing phase during mastication, the late closing phase occurs parallel to the sagittal plane (Utsumi et al., 2010). This may explain why the signature of wear on the UM1 is not impacted by the rotational component of jaw motion and is similar in all populations. However, the rate of wear may vary depending on the diet.

The commensal populations from Balan and Tourch appeared to share a rapid wear along growth, in contrast with Guillou mice and Balan laboratory offspring, displaying less advanced wear for a given growth stage, in agreement with reduced masticatory demand. The closeness between Guillou 2009 and Guillou 1993 suggest a decoupled response to loadings during mastication, impacting the insertion of the molars along the row, and to the abrasiveness of the food, affecting rate of wear.

Few highly abraded teeth, with almost all cusps worn down, appeared as outliers. Their occurrence however provides evidences that such advanced wear, and presumably age, can be occasionally reached on the Sub-Antarctic Guillou island, despite unfavorable environmental conditions and important winter mortality (Ferreira et al., 2006).

Conclusions

The present study validated the hypothesis that molar wear may trace ecological differences occurring over very short time scales. Sub-Antarctic Guillou mice display modified wear dynamics compared to commensal mice, due to their shift from an omnivorous-granivorous diet requiring efficient mastication, towards a more “predator” behavior associated with an optimization for incisor biting. In these mice, the rate of wear seems to be decreased, as in mice bred in laboratory conditions. Tracing wear dynamics requires, however, proxies of the animal’s age comparable across populations. Evolution of body size, for instance in insular populations (Gray et al., 2015), could render the comparison of wear trajectories among populations difficult. Craniofacial measurements could provide alternate proxies, but they are equally impacted by evolution and can vary depending on local conditions affecting bone mineralization, as for instance here in the early population from

Guillou (Renaud et al., 2015b). Despite these potential limits, wear trajectories could be a non-invasive approach to trace diet differences in museum specimens for which body size data are available.

Variation in the arrangement of the three molars along the row seems to trace other differences in diet, related to loadings during mastication. They were able to trace diet shifts occurring over few decades as the results of climate warming and the spread of invasive species on Guillou Island. Quantifying the torsion along the molar row could thus contribute to trace subtle diet variations, together with other proxies such as wear or topographic indices (Pampush et al., 2016). Furthermore, this approach provides a direct insight into the constraints during mastication, which may help to better understand the functional role of changes in the molar geometry.

Acknowledgements

We deeply thank contributors who collected mice from the different areas: Jean-Pierre Quéré for Tourch, Benoît Pisanu and Jean-Louis Chapuis for Guillou. People in charge of the horse stable Les Peupliers (Balan) are thanked for their authorization and support during trapping. Angéline Clair, Laetitia Averty and Julie Ulmann are warmly thanked for their investment in breeding the laboratory offspring in the animal husbandry unit ACSED. We also acknowledge the contribution of SFR Biosciences (UMS3444/CNRS, US8/Inserm, ENS de Lyon, UCBL) AniRa-ImmOs facility and the Mateis laboratory (INSA, Lyon, France), and we particularly thank Mathilde Bouchet and Justine Papillon for her kind assistance during the scanning sessions. Finally, we thank the anonymous reviewer as well as the editor, Prof. John A. Allen, for their constructive remarks on the manuscript. This work was supported by the Fédération de Recherche BioEnviS – FR3728 of University Claude Bernard Lyon 1.

Data Availability

The 3D models of most molar rows are deposited online (Renaud et al. 2023). Morphometric data are provided as Supplementary Material.

References

Adams CD, Otarola-Castillo E. 2013. geomorph: an R package for the collection and analysis of geometric morphometric shape data. *Methods in Ecology and Evolution* **4:** 393-399.

Bookstein FL. 1997. Landmark methods for forms without landmarks: morphometrics of group differences in outline shape. *Medical Image Analysis* **1:** 225-243.

Cardini A, O'Higgins P, Rohlf FJ. 2019. Seeing distinct groups where there are none: Spurious patterns from between-group PCA. *Evolutionary Biology* **46:** 303-316.

Chapuis J-L, Frenot Y, Lebouvier M. 2004. Recovery of native plant communities after eradication of rabbits from the subantarctic Kerguelen Islands, and influence of climate change. *Biological Conservation* **117:** 167-179.

Chapuis J-L, Le Roux V, Asseline J, Kerleau F. 2001. Eradication of rabbits (*Oryctolagus cuniculus*) by poisoning on three islands of the subantarctic Kerguelen Archipelago. *Wildlife Research* **28:** 323-331.

Chevret P, Hautier L, Ganem G, Herman J, Agret S, Auffray J-C, Renaud S. 2021. Genetic structure in Orkney island mice: isolation promotes morphological diversification. *Heredity* **126:** 266-278.

Cucchi T. 2008. Uluburun shipwreck stowaway house mouse: molar shape analysis and indirect clues about the vessel's last journey. *Journal of Archaeological Science* **35:** 2953-2959.

Cucchi T, Mohaseb A, Peigné S, Debue K, Orlando L, Mashkour M. 2017. Detecting taxonomic and phylogenetic signals in equid cheek teeth: towards new palaeontological and archaeological proxies. *Royal Society Open Science* **4:** 160997.

Dolédec S, Chessel D. 1987. Rythmes saisonniers et composantes stationnelles en milieu aquatique. I- Description d'un plan d'observations complet par projection de variables. *Acta Oecologica Oecologia Generalis* **8:** 403-426.

Dolédec S, Chessel D. 1994. Co-inertia analysis: an alternative method for studying species–environment relationships. *Freshwater Biology* **31:** 277-294.

Ferreira SM, Van Aarde RJ, Wassenaar TD. 2006. Demographic responses of house mice to density and temperature on sub-Antartic Marion Island. *Polar Biology* **30:** 83-94.

Ginot S, Hautier L, Agret S, Claude J. 2020. Decoupled ontogeny of in vivo bite force and mandible morphology reveals effects of weaning and sexual maturation in mice. *Biological Journal of the Linnean Society* **129:** 558–569.

Gomes Rodrigues H, Renaud S, Charles C, Le Poul Y, Solé F, Aguilar J-P, Michaux J, Tafforeau P, Headon D, Jernvall J, Viriot L. 2013. Roles of dental development and adaptation in rodent evolution. *Nature Communications* **4:** 2504.

Gómez Cano AR, Hernández Fernández M, Álvarez-Sierra MÁ. 2013. Dietary ecology of Murinae (Muridae, Rodentia): A geometric morphometric approach. *PLoS One* **8:** e79080.

Gray MM, Parmenter MD, Hogan CA, Ford I, Cuthbert RJ, Ryan PG, Broman KW, Payseur BA. 2015 Genetics of rapid and extreme size evolution in island mice. *Genetics* **201:** 213-228.

Grossnickle DM, Smith SM, Wilson GP. 2019. Untangling the multiple ecological radiations of early mammals. *Trends in Ecology and Evolution* **34:** 936-949.

Hardouin EA, Chapuis J-L, Stevens MI, van Vuuren JB, Quillfeldt P, Scavetta RJ, Teschke M, Tautz D. 2010. House mouse colonization patterns on the sub-Antarctic Kerguelen Archipelago suggest singular primary invasions and resilience against re-invasion. *BMC Evolutionary Biology* **10:** 325.

Hayden L, Lochovska L, Sémon M, Renaud S, Delignette-Muller M-L, Vicot M, Peterková R, Hovorakova M, Pantalacci S. 2020. Developmental variability channels mouse molar evolution. *eLife* **9:** e50103.

Hunter JP, Jernvall J. 1995. The hypocone as a key innovation in mammalian evolution. *Proceedings of the National Academy of Sciences, USA* **92:** 10718-10722.

Jones EP, K. S, Gibert MTP, Willerslev E, Searle JB. 2012. Fellow travellers: a concordance of colonization patterns between mice and men in the North Atlantic region. *BMC Evolutionary Biology* **12:** 35.

Kavanagh KD, Evans AR, Jernvall J. 2007. Predicting evolutionary patterns of mammalian teeth from development. *Nature* **449:** 427-432.

König B, Markl H. 1987. Maternal care in house mice. I. The weaning strategy as a means for parental manipulation of offspring quality. *Behavioral Ecology and Sociobiology* **20:** 1-9.

Laparie M, Lebouvier M, Lalouette L, Renault D. 2010. Variations of morphometric traits in populations of an invasive carabid predator (*Merizodus soledadinus*) within a sub-Antarctic island. *Biological Invasions* **12:** 3405-3417.

Lazzari V, Tafforeau P, Aguilar J-P, Michaux J. 2008. Topographic maps applied to comparative molar morphology: the case of murine and cricetine dental plans (Rodentia, Muroidea). *Paleobiology* **34:** 46-64.

Le Roux V, Chapuis J-L, Frenot Y, Vernon P. 2002. Diet of the house mouse (*Mus musculus*) on Guillou Island, Kerguelen archipelago, Subantarctic. *Polar Biology* **25:** 49-57.

Lebouvier M, Chapuis J-L, Gloaguen J-C, Frenot Y. 2002. Résilience des communautés insulaires subantarctiques: facteurs influençant la vitesse de restauration écologique après éradication de mammifères introduits. *Revue d'Ecologie (Terre Vie)* **supplément 9:** 189-198.

Lebrun R. 2018. MorphoDig, an open-source 3D freeware dedicated to biology. . IPC5, 5th International Palaeontological Congress. Paris, France.

Ledevin R, Chevret P, Ganem G, Britton-Davidian J, Hardouin EA, Chapuis J-L, Pisanu B, Mathias MdL, Schlager S, Auffray J-C, Renaud S. 2016. Phylogeny and adaptation shape the teeth of insular mice. *Proceedings of the Royal Society of London, Biological Sciences (serie B)* **283:** 20152820.

Maejima M, Abe S, Sakiyama K, Agematsu H, Hashimoto M, Tamatsu Y, Ide Y. 2005. Changes in the properties of mouse tongue muscle fibres before and after weaning. *Archives of Oral Biology* **50:** 988-993.

Miller AP, Webb PI. Diet of house mice (*Mus musculus* L.) on coastal sand dunes, Otago, New Zealand. *New Zealand Journal of Zoology* **28:** 49-55.

Pallares LF, Ledevin R, Pantalacci S, Turner LM, Steingrimsson E, Renaud S. 2017. Genomic regions controlling shape variation in the first upper molar of the house mouse. *eLife* **6:** e29510.

Pampush JD, Spradley JP, Morse PE, Harrington AR, Allen KL, Boyer DM, Kay RF. 2016. Wear and its effects on dental topography measures in howling monkeys (*Alouatta palliata*).

Pocock MJO, Searle JB, White PCL. 2004. Adaptations of animals to commensal habitats: population dynamics of house mice *Mus musculus domesticus* on farms. *Journal of Animal Ecology* **73:** 878-888.

Renaud S, Auffray J-C, de La Porte S. 2010. Epigenetic effects on the mouse mandible: common features and discrepancies in remodeling due to muscular dystrophy and response to food consistency. *BMC Evolutionary Biology* **10:** 28.

Renaud S, Dufour A-B, Hardouin EA, Ledevin R, Auffray J-C. 2015a. Once upon multivariate analyses: when they tell several stories about biological evolution. *PLoS One* **10:** e0132801.

Renaud S, Gomes Rodrigues H, Ledevin R, Pisanu B, Chapuis J-L, Hardouin EA. 2015b. Fast morphological response of house mice to anthropogenic disturbances on a Sub-Antarctic island. *Biological Journal of the Linnean Society* **114:** 513-526.

Renaud S, Hardouin EA, Pisanu B, Chapuis J-L. 2013. Invasive house mice facing a changing environment on the Sub-Antarctic Guillou Island (Kerguelen Archipelago). *Journal of Evolutionary Biology* **26:** 612-624.

Renaud S, Hardouin EA, Quéré J-P, Chevret P. 2017. Morphometric variations at an ecological scale: Seasonal and local variations in feral and commensal house mice. *Mammalian Biology* **87:** 1-12.

Renaud S, Ledevin R. 2017. Impact of wear and diet on molar row geometry and topography in the house mouse. *Archives of Oral Biology* **81:** 31-40.

Renaud S, Ledevin R, Pisanu B, Chapuis J-L, Quillfeldt P, Hardouin EA. 2018a. Divergent in shape and convergent in function: adaptive evolution of the mandible in Sub-Antarctic mice. *Evolution* **72:** 878-892.

Renaud S, Ledevin R, Romestaing C, Hardouin EA. 2023. 3D models related to the publication: "Molar wear in house mice: insight into diet preferences at an ecological time scale?". *MorphoMuseuM***:** e200. doi: 10.18563/journal.m3.200

687 **Renaud S, Ledevin R, Souquet L, Gomes Rodrigues H, Ginot S, Agret S, Claude J, Herrel A, Hautier L.**
688 **2018b.** Evolving teeth within a stable masticatory apparatus in Orkney mice. *Evolutionary*
689 *Biology* **45:** 405-424.
690 **Renaud S, Pantalacci S, Auffray J-C. 2011.** Differential evolvability along lines of least resistance of
691 upper and lower molars in island house mice. *PLoS One* **6:** e18951.
692 **Renaud S, Romestaing C, Savriama Y. 2021.** 3D models related to the publication: Wild vs lab house
693 mice: effects of age, diet and genetics on molar geometry and topography. *MorphoMuseuM*
694 **7:** e141.
695 **Savriama Y, Romestaing C, Clair A, Averty L, Ulmann J, Ledevin R, Renaud S. 2022.** Wild versus lab
696 house mice: Effects of age, diet, and genetics on molar geometry and topography. *Journal of*
697 *Anatomy* **240:** 66-83.
698 **Schlager S. 2017.** Chapter 9. Morpho and Rvcg - Shape Analysis in R: R-Packages for Geometric
699 Morphometrics, Shape Analysis and Surface Manipulations,. In: Zheng G, Li S and Székely G,
700 eds. *Statistical shape and deformation analysis*: Academic Press. 217-256.
701 **Swiderski DL, Zelditch ML. 2013.** The complex ontogenetic trajectory of mandibular shape in a
702 laboratory mouse. *Journal of Anatomy* **223:** 568-580.
703 **Teaford MF, Oyen OJ. 1989.** Differences in the rate of molar wear between monkeys raised on
704 different diets. *Journal of Dental Research* **68:** 1513-1518.
705 **Thioulouse J, Dray S, Dufour A-B, Siberchicot A, Jombart T, Pavoine S. 2018.** *Multivariate Analysis of*
706 *Ecological Data with ade4.* Springer.
707 **Thioulouse J, Renaud S, Dufour A-B, Dray S. 2021.** Overcoming the spurious groups problem in
708 between-group PCA. *Evolutionary Biology* **48:** 458-471.
709 **Utsumi D, Nakamura A, Matsuo K, Zeredo JL, Koga Y, Yoshida N. 2010.** Motor coordination of
710 masseter and temporalis muscle during mastication in mice. *International Journal of*
711 *Stomatology and Occlusion Medicine* **3:** 187-194.
712 **Weissbrod L, Marshall FB, Valla FR, Khalaily H, Bar-Oz G, Auffray J-C, Vigne J-D, Cucchi T. 2017.**
713 Origins of house mice in ecological niches created by settled hunter-gatherers in the Levant
714 15,000 y ago. *Proceedings of the National Academy of Sciences, USA* **114:** 4099-4104.

715

716

Tables

	P_{KW}	BW/BL	BW/G09	BW/G93	BW/To	BL/G09	BL/G93	BL/To	G09/G93	G09/To	G93/To
$BWeight^{1/3}$	0.0692	0.538	1.000	1.000	1.000	1.000	1.000	0.077	1.000	0.743	0.743
MdL	*0.0037*	0.079	1.000	0.364	1.000	0.454	0.012	0.079	0.267	1.000	0.394
UM1 CS	**<0.0001**	0.086	*0.003*	0.341	0.526	**0.0002**	0.041	0.526	0.526	**0.0001**	0.040

Table 1. Size differences between populations. PKW: Kruskal-Wallis probability; next columns: probabilities of pairwise differences (Wilcoxon test). $BWeight^{1/3}$: cubic root of body weight; MdL: mandible length; UM1 CS: centroid size of the first upper molar. In bold, P < 0.001. In italics P < 0.01 (uncorrected P-values are provided). BW: Balan Wild; BL: Balan Lab; G93: Guillou 93; G09: Guillou 09; To: Tourch.

		Age	Sex	Age:Sex
Anova	$BWeight^{1/3}$	**0.0001**	0.0836	0.1719
	MdL	**0.0001**	0.6989	0.7897
ProcD.lm	UMR	**0.0003**	0.3146	0.0857
	UM1	**0.0001**	0.4607	0.5812

Table 2. Effect of age and sex on body size proxies and wear trajectories. $BWeight^{1/3}$: cubic root of body weight ; MdL: Mandible length. In bold P < 0.001.

	$BW^{1/3}$						MdL					
	%	P					%	P				
UMR	6.9	**0.0003**					6.6	**0.0005**				
UM1	7.2	**0.0005**					10.6	**0.0001**				
UM1tr	1.0	0.8316					2.5	0.0861				
	CRW		Gp		W:Gp		MdL		Gp		MdL:Gp	
	%	P	%	P	%	P	%	P	%	P	%	P
UMR	6.9	**0.0001**	33.2	**0.0001**	4.8	0.1696	6.6	**0.0001**	33.5	**0.0001**	5.2	0.0686
UM1	7.2	**0.0001**	33.4	**0.0001**	4.9	0.1497	10.6	0.0001	28.9	**0.0001**	4.5	0.2970
UM1tr	1.0	0.5656	29.6	**0.0001**	5.5	0.1779	2.5	0.0171	28.6	**0.0001**	6.3	0.3820

Table 3. Relationships between shape (aligned coordinates) and proxy of animal's size and populations. Percentage of variance explained (%) and probabilities (P) of Procrustes ANOVA are given. $BW^{1/3}$: cubic root of body weight. MdL: mandible length. In bold P < 0.001, in italics P < 0.01.

733 **Figures and Figure Captions**

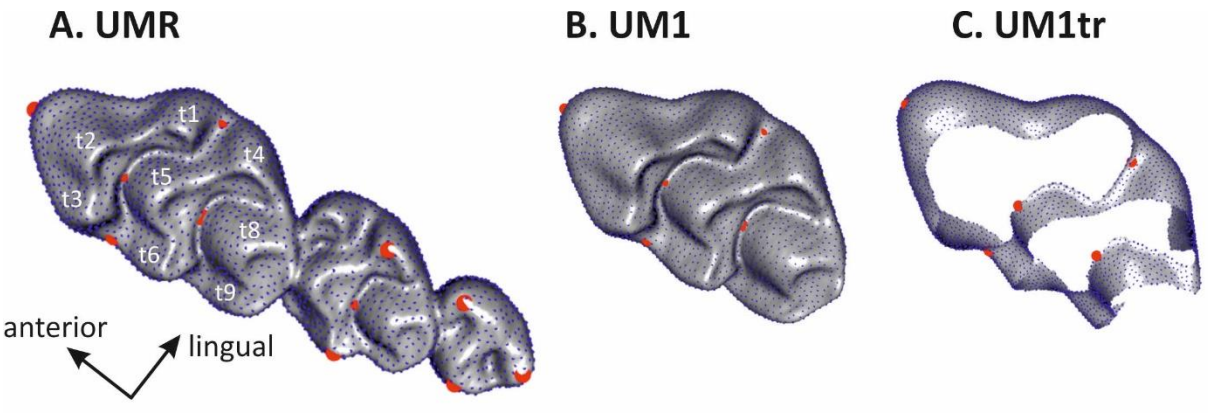

734

735 *Figure 1. Templates used to describe the 3D molar morphology. (A) Upper molar row (UMR), with*
736 *labelling of the cusps. (B) First upper molar (UM1). (C) Truncated "wear-free" first upper molar*
737 *(UM1tr). Red dots: fixed landmarks used to anchor the templates; blue dotes: sliding semi-landmarks.*

738

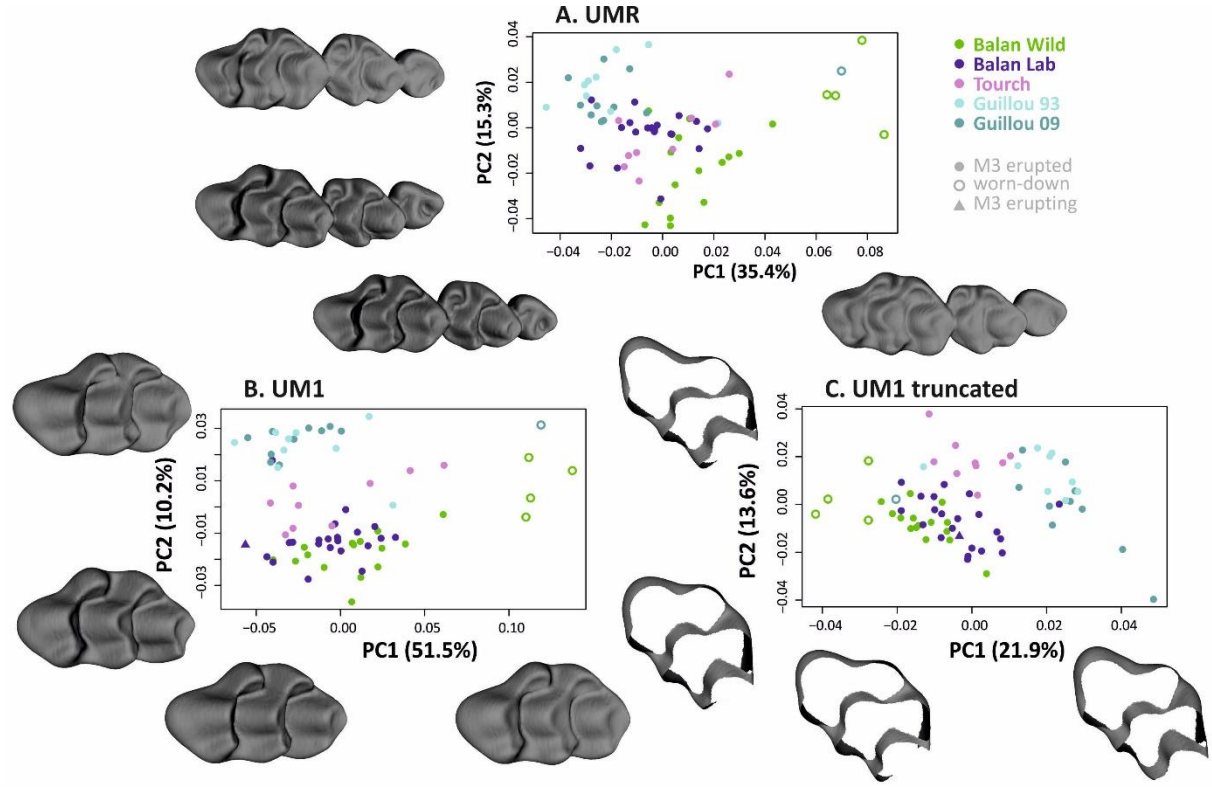

739

740 *Figure 2. Morphospaces depicting the shape variation of the upper molar row (A), the first upper*
741 *molar (B) and the truncated first upper molar (C). The first two axes of a PCA on the aligned*
742 *coordinates are represented. Along each axis, visualizations of molar shape corresponding to PC*
743 *scores = 0.05 and -0.05 are depicted. Top right: legend common to the three panels (specimen with*
744 *M3 erupting absent from the analysis of the UMR on panel A).*

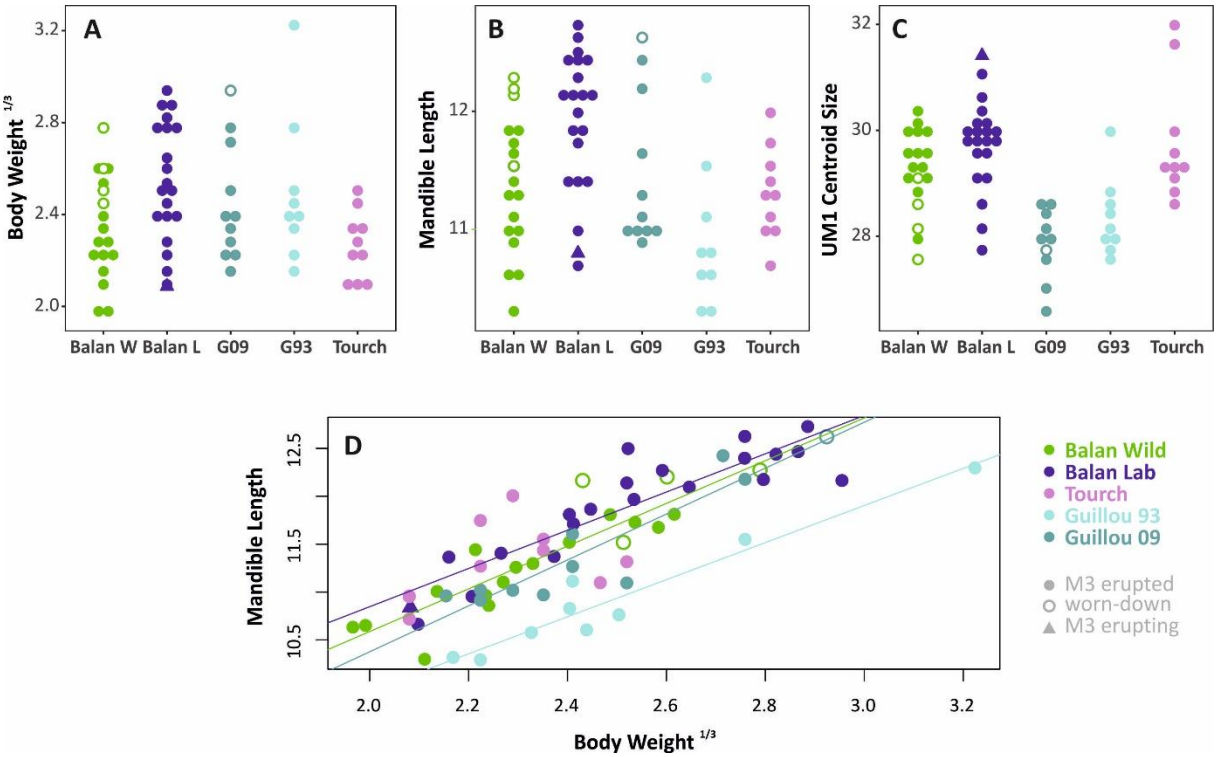

745

746 *Figure 3. Size differences between populations and relationship between size estimators. (A) cubic*
747 *root of body weight. (B) mandible length. (C) centroid size of the first upper molar. (D) Relationship*
748 *between body weight$^{1/3}$ and mandible length. Full lines represent significant within-population*
749 *regressions (P < 0.05).*

750

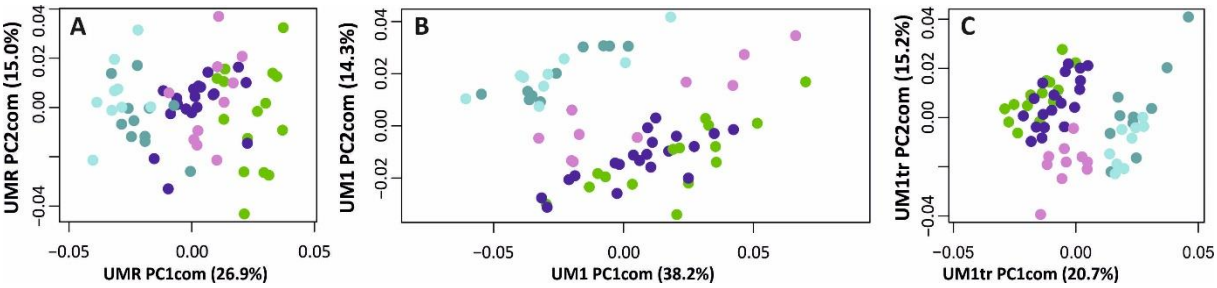

751

752 *Figure 4. Morphospaces representing shape variation of the upper molar row (A), the first upper*
753 *molar (B) and the truncated first upper molar (C), corresponding to PCAs on a subsampling (N = 64)*
754 *discarding the senescent specimens and the mouse at weaning.*

755

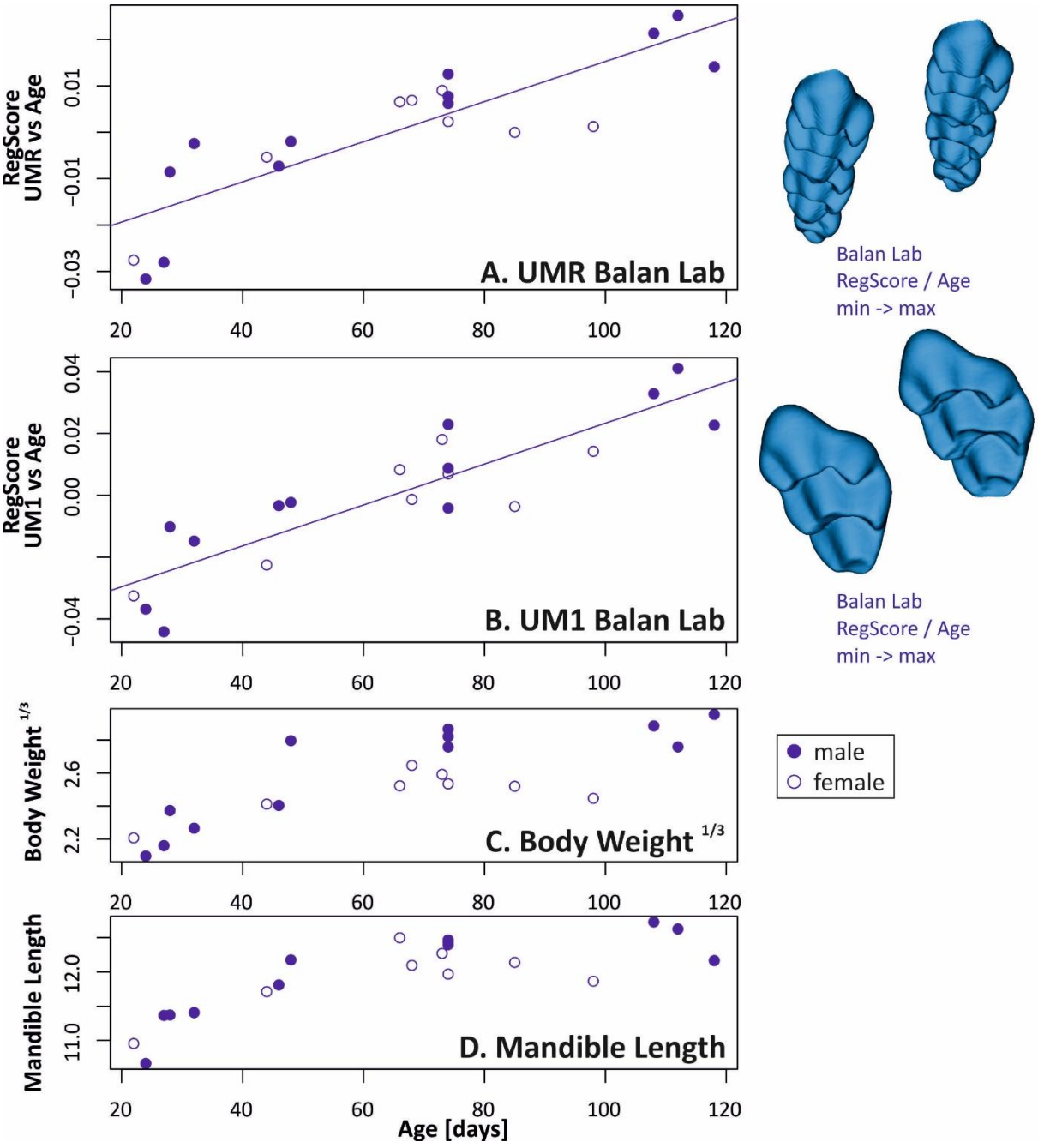

Figure 5. Variations with age and sex in the group of laboratory-bred mice (Balan Lab). (A,B) Wear trajectories as a function of age, visualized using regression scores based on Procrustes ANOVAs of aligned coordinates of the upper molar row (A) and the first upper molar (B). Full lines represent the regression of regression score vs. age ($P < 0.05$). (C) Body weight$^{1/3}$ as a function of age in the same mice. (D) Mandible length as a function of age. The symbols correspond to the sex of the mice.

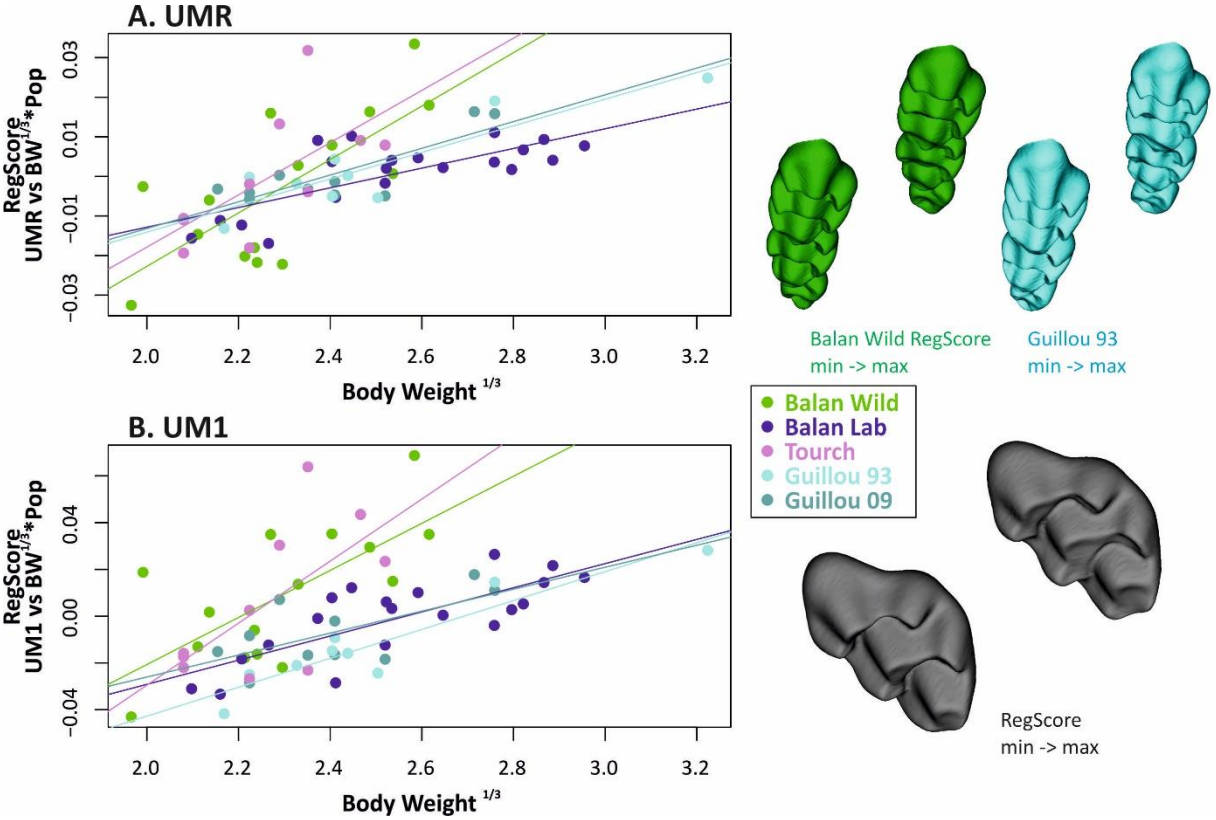

763

764 *Figure 6. Wear trajectories for the upper molar row (A) and the first upper molar (B). Body weight$^{1/3}$ is*
765 *used as proxy of growth. Regression scores, based on Procrustes ANOVAs of aligned coordinates vs*
766 *body weight$^{1/3}$ and population, allowed to visualize shape variance related to wear within each*
767 *group. Full lines represent significant within-group regressions of regression score vs. weight$^{1/3}$*
768 *(significant within all groups at $P < 0.05$).*

769

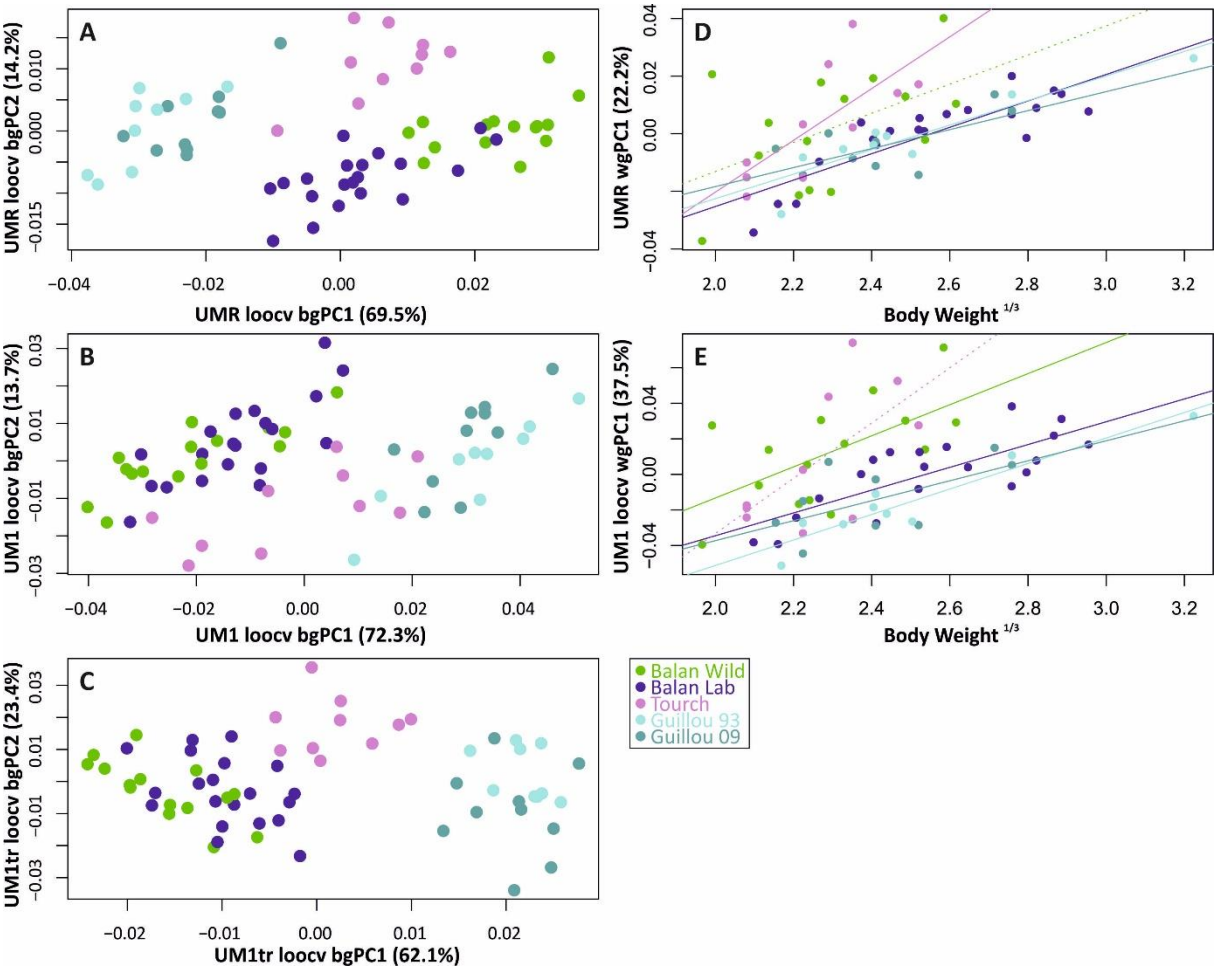

Figure 7. Between-group variation (A,B,C) and within-group variation (D,E) of the molar geometry. (A,D) Upper molar row; (B,E) first upper molar; (C) truncated first upper molar. (A, B, C) Cross-validated factor map of the bgPCA. (D, E) Relationship between the first within-group PC axis and body weight$^{1/3}$. Full lines correspond to significant within-group regressions ($P < 0.05$). The dotted line corresponds to marginally significant regression ($0.05 < P < 0.10$).

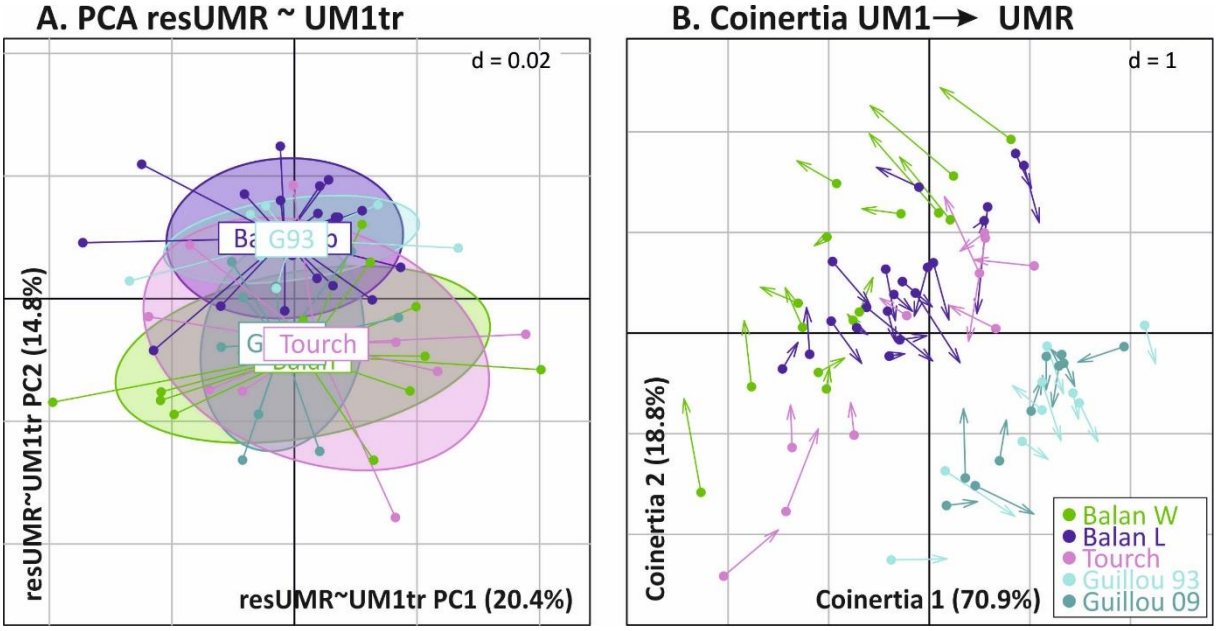

777

778 *Figure 8. (A) PCA on the residuals of a multivariate regressions of the UMR aligned coordinates vs the*
779 *first two axes of the PCA on the truncated UM1. (B) Coinertia between shape variation of the UM1*
780 *and UMR. The arrow indicates the change in topology going from the first (UM1) to the second (UMR)*
781 *dataset.*

782

783

Supplementary Material

Supplementary Figure 1. Map of the localities considered in the study.

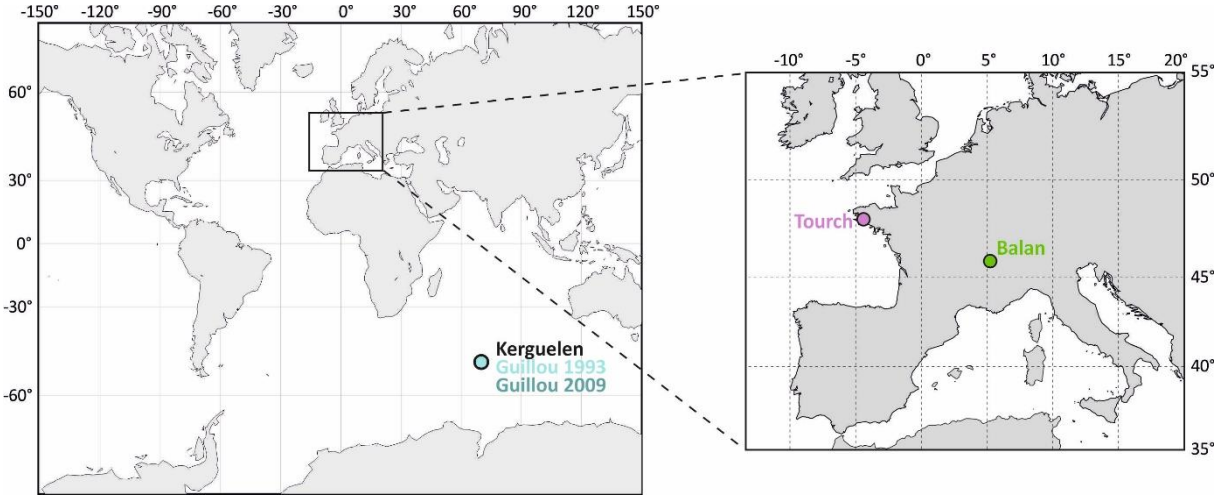

Supplementary Table 1. Sampling of the study: Specimen ID, population, wear stage, age for laboratory specimens, weight and 3D mandible length.

Individual ID	Population	Stage	Age [days]	Sex	Weight [g]	MdL [mm]
Balan_02_2015	Balan	adult			7.6	10.6
Balan_03	Balan	adult		F	12.1	11.3
Balan_04	Balan	senescent		F	21.7	12.3
Balan_06	Balan	adult		M	17.9	11.8
Balan_07	Balan	adult		F	11.3	10.9
Balan_08	Balan	adult		F	17.3	11.7
Balan_11	Balan	adult		M	10.9	11.4
Balan_12	Balan	adult		F	11.7	11.1
Balan_BAL15	Balan	adult		M	11.2	11.0
Balan_BAL16	Balan	senescent		M	15.9	11.5
Balan_BAL17	Balan	adult		M	7.9	10.7
Balan_BAL18	Balan	adult		F	9.4	10.3
Balan_BAL19	Balan	adult		M	16.3	11.7
Balan_BAL20	Balan	adult		M	12.7	11.3
Balan_BAL21	Balan	senescent		M	17.6	12.2
Balan_BAL22	Balan	adult		F	13.9	11.5
Balan_BAL23	Balan	adult		F	15.4	11.8
Balan_BAL24	Balan	senescent		M	14.4	12.2
Balan_BAL25	Balan	adult		M	9.8	11.0
Balan_Lab_35	BalanLab	adult	98	F	14.7	11.9
Balan_Lab_46	BalanLab	adult	85	F	16.0	12.1
Balan_Lab_54	BalanLab	adult	73	F	17.4	12.3
Balan_Lab_56	BalanLab	adult	74	F	16.3	12.0

Balan_Lab_86	BalanLab	adult	108	M	24.0	12.7
Balan_Lab_82	BalanLab	adult	118	M	25.8	12.2
Balan_Lab_92	BalanLab	adult	112	M	21.0	12.6
Balan_Lab_319	BalanLab	adult	68	F	18.5	12.1
Balan_Lab_325	BalanLab	adult	74	M	22.5	12.4
Balan_Lab_329	BalanLab	adult	74	M	21.0	12.4
Balan_Lab_330	BalanLab	adult	74	M	23.6	12.5
Balan_Lab_02050407_01	BalanLab	adult	63	F		12.4
Balan_Lab_17032205_01	BalanLab	adult	66	F	16.1	12.5
Balan_Lab_BB3weeks	BalanLab	weaning	21		9.0	10.8
Balan_Lab_167	BalanLab	adult	48	M	21.9	12.2
Balan_Lab_188	BalanLab	adult	32	M	11.6	11.4
Balan_Lab_192	BalanLab	adult	28	M	13.4	11.4
Balan_Lab_194	BalanLab	adult	46	M	13.9	11.8
Balan_Lab_196	BalanLab	adult	44	F	14.0	11.7
Balan_Lab_30x17	BalanLab	adult	27	M	10.1	11.4
Balan_Lab_40x56	BalanLab	adult	24	M	9.2	10.7
Balan_Lab_47x61	BalanLab	adult	22	F	10.8	11.0
G09_06	G09	adult		F	10.0	11.0
G09_10	G09	adult		F	16.0	11.1
G09_15	G09	adult		F	11.0	11.0
G09_16	G09	adult		M	14.0	11.3
G09_17	G09	adult		M	11.0	10.9
G09_21	G09	adult		F	21.0	12.2
G09_26	G09	senescent		M	25.0	12.6
G09_27	G09	adult		F	20.0	12.4
G09_29	G09	adult		F	13.0	11.0
G09_65	G09	adult		M	14.0	11.6
G09_66	G09	adult		M	12.0	11.0
G93_03	G93	adult		F	12.6	10.6
G93_04	G93	adult		F	11.0	10.3
G93_10	G93	adult		F	15.7	10.8
G93_11	G93	adult		M	14.5	10.6
G93_13	G93	adult		F	14.0	11.1
G93_14	G93	adult		F	13.9	10.8
G93_15	G93	adult		F	10.2	10.3
G93_24	G93	adult		M	21.0	11.6
G93_25	G93	adult		M	33.5	12.3
Tourch_7819	Tourch	adult		F	12.0	12.0
Tourch_7821	Tourch	adult		F	11.0	11.7
Tourch_7839	Tourch	adult		M	9.0	11.0
Tourch_7873	Tourch	adult		M	13.0	11.6
Tourch_7877	Tourch	adult		F	11.0	11.3
Tourch_7922	Tourch	adult		M	15.0	11.1
Tourch_7923	Tourch	adult		F	16.0	11.3
Tourch_7925	Tourch	adult		M	13.0	11.4

Tourch_7927	Tourch	adult		F	9.0	11.0
Tourch_7932	Tourch	adult		M	9.0	10.7

790

791

792 **Supplementary Files (datasets)**

793 UM1_BWLGT_BJLS_Renaud_et_al_2023.txt

794 File containing for each specimen (IndID) the population, centroid size (CS) and PC scores
795 corresponding to the UM1 analysis.

796

797 UM1tr_BWLGT_BJLS_Renaud_et_al_2023.txt

798 File containing for each specimen (IndID) the population, centroid size (CS) and PC scores
799 corresponding to the analysis of the truncated UM1.

800

801 UMR_BWLGT_BJLS_Renaud_et_al_2023.txt

802 File containing for each specimen (IndID) the population, centroid size (CS) and PC scores
803 corresponding to the UMR analysis. Note that corresponding to the previous files, the specimen at
804 weaning (Balan_Lab_BB3weeks) has been deleted since its molar row was not complete (eruption of
805 the UM3 not completed).

806

807

808

809